Probiotics and Antimicrobial Proteins (2022) 14:180–188
https://doi.org/10.1007/s12602-022-09910-y

Antimicrobial Peptides from Human Microbiome Against Multidrug Efflux Pump of *Pseudomonas aeruginosa*: a Computational Study

Viswajit Mulpuru[1] **· Nidhi Mishra**[1]

Accepted: 9 January 2022 / Published online: 17 January 2022

Abstract
The excess use of antibiotics has led to the evolution of multidrug-resistant pathogenic strains causing worldwide havoc. These multidrug-resistant strains require potent inhibitors. *Pseudomonas aeruginosa* is a lead cause of nosocomial infections and also feature in the critical priority list of the world health organization (WHO) for the development of new antibiotics against their antimicrobial resistance. Antimicrobial peptides (AMPs) found in almost every life form from microorganisms to humans are known to defend their hosts against various pathogens. Owing to the diversity of the human microbiome, in this study, we have identified the cell-penetrating AMPs from the human microbiome and studied their inhibitory activity against the outer membrane protein OprM of the MexAB–OprM, a constitutively expressed multidrug efflux pump of the *Ps. aeruginosa*. Screening of the AMPs from the human microbiome resulted in the identification of 147 cell-penetrating AMPs (CPAMPs). The virtual screening of these CPAMPs against the OprM protein showed significant inhibitory results with the top docked AMP showing binding affinity exceeding −30 kcal/mol. The molecular dynamic simulation determined the interaction stabilities between the AMPs and the OprM at the binding site. Further, the residue interaction networks (RINs) are analyses to identify the inhibitory patterns. Later, these patterns were confirmed by MM-PBSA analysis suggesting that the AMPs are majorly stabilized by electrostatic interactions at the binding site. Thus, the high binding affinity and insights from the molecular interaction signify that the identified CPAMPs from the human microbiome can be further explored as inhibitory agents against multidrug-resistant *Ps. aeruginosa.*

Keywords Antimicrobial peptides · Human microbiome · Efflux pumps · Multidrug resistance · AMP · MDR

Introduction

The twentieth-century, golden age of the antibiotic era has witnessed the discovery of about half of the antibiotics used today helping cure dreadful bacterial infections saving millions if not billions of lives. Speaking of life, survival of the fittest has always played a prominent role in evolution. Due to the misuse and abuse of antibiotics, the disease-causing microbes rapidly evolved to survive the antibiotic use resulting in the emergence of antibiotic and multidrug-resistant bacterial strains. According to a recent UN committee report, about 700,000 people die each year globally due to drug-resistant bacteria. By 2030, it is estimated that drug-resistant bacterial strains may kill up to 10 million people each year threatening us of a post-antibiotic era where a minor infection could prove deadly. The recent report of WHO also states that the development of new antibiotics against antimicrobial-resistant *Acinetobacter baumannii, Pseudomonas aeruginosa,* and *Enterobacteriaceae* is of critical priority.

Adding to this, the shocking fact of pharmaceutical industries losing enthusiasm in developing antibiotics due to the rapid development of antibiotic resistance by bacteria will surely send chills through our spine. Given this, to combat antibiotic resistance, researchers are targeting the bacterial mechanism of antibiotic resistance. It is studied that the four major mechanisms of antibiotic resistance in a bacterial cell are (i) altering the cellular permeability to prevent the entry of antibiotics, (ii) modifying the antibiotic targets to render them to be ineffective, (iii) inactivating the antibiotics through enzymatic action, and (iv) expression or overexpression of efflux pumps to pump out antibiotics [1].

✉ Nidhi Mishra
nidhimishra@iiita.ac.in

[1] Department of Applied Sciences, Indian Institute of Information Technology Allahabad, Prayagraj, India

Classified into six families, namely, the ATP-binding cassette (ABC) superfamily, the major facilitator superfamily (MFS), the multidrug and toxic compound extrusion (MATE), the small multidrug resistance (SMR) family, the resistance-nodulation-division (RND) superfamily, and the drug metabolite transporter (DMT) superfamily [2], it is studied that efflux pumps constitute the most ubiquitous type of antimicrobial resistance in all organisms [3, 4].

Coming to the innate antimicrobial resistance, almost all the organisms from simple single cellular to complex multicellular microbes produce antimicrobial peptides (AMPs) showing innate defense activities [5]. Studies suggest these AMPs are known to show high potency towards antibacterial activity with functions ranging from wound healing to immune modulation [6].

With *P. aeruginosa* being a leading cause of nosocomial infections amounting to about 10% of all hospital-acquired infections [7, 8], In this study, we focus on the identification of inhibitors for the efflux pumps that act as determinants of resistance from bacterial strain *Ps. aeruginosa* using antimicrobial peptides through an in-silico approach. Owing to the diverse ecological community of the human microbiome, we considered the AMPs from the human microbiome that was identification in a recent study to inhibit the drug-resistant *P. aeruginosa* [9].

As it is known that the RND superfamily of efflux pumps plays an important role in multidrug resistance [10], three outer membrane proteins, namely, OprM, OprJ, and OprN are identified to be responsible for multiple drug resistance in *P. aeruginosa* [11]. Of these three known outer membrane proteins, OprM is the only known protein to be constitutively expressed in *P. aeruginosa* contributing significantly to its antimicrobial resistance [12, 13].

Considering the above, we have used the three-dimensional structure of OprM protein to predict its potential inhibitors from AMPs identified from human metagenome using an in-silico approach.

Materials and Methods

Protein Structure Identification

The protein structure of the multidrug efflux pump of *Ps. aeruginosa* was retrieved from the protein data bank (PDB). The OprM structure was extracted from the co-crystallized X-ray structure of the outer membrane protein OprM with multidrug resistance protein MexA and multidrug resistance protein MexB (PDB ID: 6IOL). This extracted OprM structure is considered as the target for the virtual screening of the AMPs using in-silico studies for identifying its potential inhibitory peptides.

Identification of AMPs

It is studied that peptides less than 30 amino acids are considered to be cell-penetrating peptides (CPPs) [14, 15]. All the AMPs containing 30 or fewer amino acids from the HAMP database [9] amounting to 147 AMPs are identified and extracted for this study. These 147 AMPs were subject to molecular docking studied to identify their interactions and inhibitory effects on the outer membrane protein OprM of *Ps. aeruginosa*.

Molecular Docking

To identify the potential peptide inhibitors of the outer membrane protein OprM, it was subjected to docking studies against the potential cell-penetrating AMPs (CPAMPs). As the binding pocket of the peptides on the protein is not previously known, the binding pocket affinity maps of the protein were generated and selected using AutoGridFR [16]. AutoGridFR is a binding site prediction tool from the AutoDockFR, AutoDock4, and AutoDock CrankPep suites. Further, the CPAMPs are docked onto the OprM at the identified active site grid coordinates using AutoDock CrankPep (ADCP) [17], a docking engine specialized for peptides docking based on CRANKITE [18] using a modified Metropolis Monte Carlo algorithm. ADCP works with the affinity maps of the AutoDock to identify the potential energy landscape of the receptor. Using this energy landscape, the peptides are folded to yield the docked poses of the peptide at the grid site. As it is known that the larger the peptide, the larger the Monte Carlo steps required, we performed 100 independent searches per peptide with 30 million Monte Carlo evaluation steps per search allocating about 1 million steps per amino acid in the peptide. Each search is performed by randomly rotating and placing a constructed peptide structure from the amino acid sequence in the identified docking grid box with a 4-Å padding on each side.

Molecular Dynamic Simulation

The top three docked peptide structures from the docking studies are subjected to molecular dynamics simulation analysis to explore their stability and conformational flexibility using CHARMM36 all-atom force field (March 2019) [19] and GROMACS (Version 2018.2) [20]. Inhouse ad hoc scripts were used to generate GROMACS compatible files before the topologies were solvated, minimized, and equilibrated. The protein-peptide complexes are solvated using TIP3P explicit water molecules, and the system was neutralized using Cl− and Na+ ions as needed. The complex

was minimized until the maximum force is less than 10.0 kJ/mol using particle Mesh Ewald summation [21] by the steepest descent algorithm. Further, The NVT and NPT conserved ensembles were used to equilibrate the system by Berendsen thermostat and Berendsen pressure coupling [22], respectively, at constant pressure and temperature of 1 bar and 310 K with a simulation time of 100 ps for each. After equilibration, molecular dynamic simulations of 50 ns were performed for each protein-peptide complex at constant temperature and pressure of 310 K and 1 bar, respectively, using the leapfrog algorithm with an integration time step of 2 fs. The trajectory was saved every 30 ps. Further, the generated trajectories were analyzed using GROMACS analytic utilities to conclude results. The root-mean-square deviation (RSMD) between the initial and the simulated structure, the radius of gyration (Rg), change in coulombic interaction energies, and hydrogen bonding between the outer membrane protein and the peptide over the simulation time are evaluated to determine the stability of the docked complexes. Further, the free energy landscape (FEL) analysis was performed along the principal components PC1 and PC2 of essential dynamics projections [23] to evaluate the conformational stability of the complex.

Binding Free Energy (MM-PBSA) Analysis

The residue interaction-energy-based investigation of the MD simulations is used to estimate the binding free energy of the protein-phytochemical complexes. The binding free energy helps in determining the interaction stability of the peptide at the binding site. The residue interaction energy between the protein and the peptide residues (ΔG_{bind}) can be stated as

$$\Delta G_{\text{bind}} = \Delta E_{\text{MM}} + \Delta G_{\text{sol}}$$

where ΔE_{MM} and ΔG_{sol} signify the deviations of the molecular mechanics and solvation free energy due to ligand binding. The Poisson Boltzmann and surface area-based approach were used to calculate the polar and non-polar solvation energies, respectively [24].

Determining the Maximum Common Substructure

The conformation of a protein inhibitor can be predicted by aligning it with the three-dimensional structure of a reference inhibitor molecule. Commonly known as similarity-based docking, this method determines the one-on-one atomic correspondence between two molecular structures helping in identifying compounds with similar biological activities [25]. In this study, we have identified the MCS between the top docked structures to determine the most prominent molecular conformation and molecular residues that determine the inhibitory effect on the outer membrane protein OprM at the identified binding pocket.

To find the most prominent protein and peptide residues involved in the interaction, firstly, the RINalyzer [26] and Cytoscape 3.8.0 [27] are used to generate the residue interaction networks (RIN) of the five best-docked peptides with the protein structure. These RINs are analyzed to determine the most common protein residues that could play a prominent role in inhibitory activity. Later, to identify the important peptide residues involved in antimicrobial activity, the MCS between the RINs of the three best-docked peptides are generated using CytoMCS [28]. The patterns of the peptide residues involved in forming the MCS are analyzed and further validated using free energy analysis results to identify the most significant pattern of AMPs involved in inhibition.

Results

Molecular Docking

The outer membrane protein OprM that plays an important role in drug resistance in *Ps. aeruginosa* is subjected to docking studies against antimicrobial peptides to identify its potential inhibitor that aids in controlling drug-resistance superbugs. The antimicrobial peptides identified from the human metagenome are used in docking studies. The docking studies reveal that these antimicrobial peptides show significant inhibitory activity against the multidrug-resistant efflux pump.

With the best-docked peptide showing a binding affinity of −30.9 kcal/mol, and an average binding affinity of 28.5 kcal/mol for the top ten docked peptides, it is considered that these peptides show significant inhibitory activity against the multi-drug resistance in *Ps. aeruginosa*. The binding affinities of the top ten AMPs as predicted by AutoDock CrankPep are given in Table 1 along with their HAMP

Table 1 Molecular docking scores (kcal/mol) of the AMPs from the Human Microbiome (best 10 hit molecules) with the drug-resistant outer membrane protein OprM

HAMP ID	Affinity (kcal/mol)
862	−30.9
834	−30.4
1298	−29.8
1518	−28.8
232	−28.7
309	−28.7
2397	−27.6
1104	−26.8
2311	−26.7
2997	−26.3

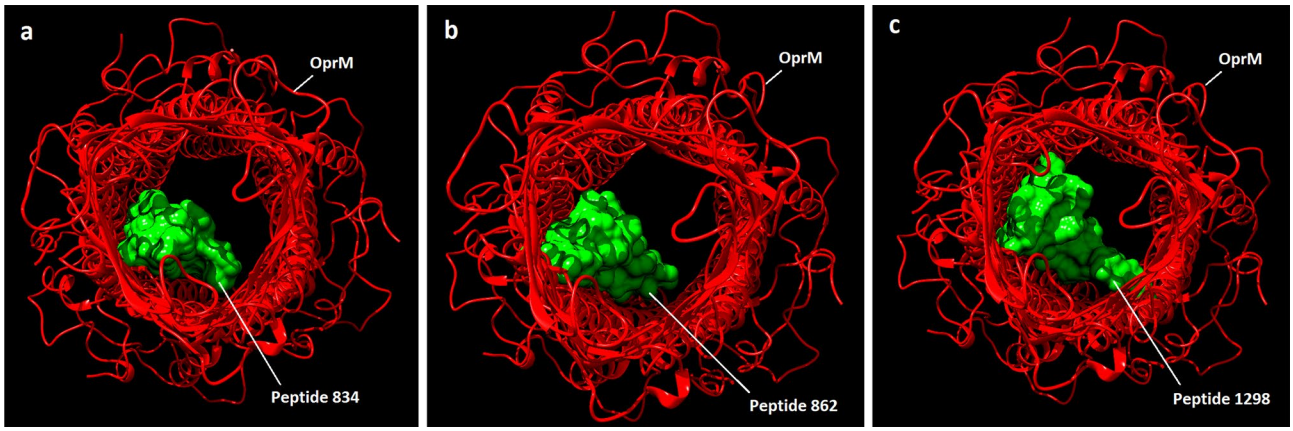

Fig. 1 Molecular docking analysis of the CPAMPs blocking the outer membrane protein OprM of the multidrug efflux pump MexAB-OprM from *Pseudomonas aeruginosa.* (**a**) 834, (**b**) 862, and (**c**) 1298

knowledgebase identifier and the structural conformations of the top three docked structures are shown in Fig. 1.

Although the docking results suggest that the AMPs could play an important role in inhibiting multidrug resistance, considering the assumptions during docking studies such as rigidity of the receptor and binding site for fast screening of the peptides along with overlooking the dynamics of the interaction between the protein and the AMPs, MD simulations of the docked complexes are performed mimicking the flexibility of the protein and peptides for a more realistic quantum level interaction studies with reference to time.

Molecular Dynamics

The conformational stability of the top three docked protein-peptide complexes was assessed by molecular dynamics simulation of 50 ns using various structural order parameters such as RMSD, Rg, and H-bond interactions. On comparing the Cα-RMSD of the peptide from the OprM-AMP complexes, it is observed that all the AMPs achieved stability at the active site rapidly (Fig. 2a). These OprM-AMP complexes attained stability in about 10 ns without any major deviations throughout the simulation time. The RMSD plot of 834 shows an initial rise in RMSD of ~0.7 nm and settles rapidly showing stable conformation for the whole 50 ns, suggesting stable interaction of 834 with outer membrane protein OprM. The trajectory of 1298 with OprM shows a slightly greater initial deviation of ~0.8 nm but this complex too settled rapidly showing a stable interacting conformation for the whole simulation time. Notably, the conformational dynamics of 862 with OprM are observed up be very stable with a low initial deviation of ~0.5 nm. This rapid equilibration of the peptides indicates their interaction stability. The stable trajectories of the peptides during 100 ns simulation time indicate that the AMPs are spatially stable at the active site of OprM.

To further investigate the conformational stability of the OprM-AMP complexes, the radius of gyration (Rg) has been analyzed to check the structure compactness. With an average Rg of 1.54 nm, 1.48 nm, and 1.30 nm for AMPs

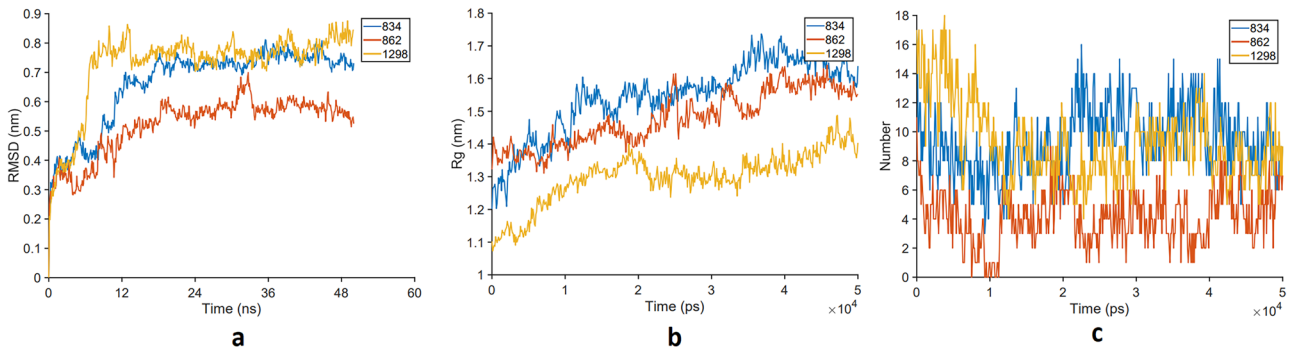

Fig. 2 Time evolution plot of the structural order parameters of the AMPs with target protein OprM. **a** The RMSD of peptide Cα-atoms, **b** radius of gyration (Rg) of the peptide, and **c** the propensity of H-bonds interaction between the AMPs and the protein during the period of simulation (100 ns) at 300 K

834, 862, and 1298, respectively, the structural integrity of the peptides remains stable throughout the simulation time (Fig. 2b). The small initial deviations in the Rg suggest minor conformational rearrangement of the peptide in the binding site of OprM.

To further understand the interaction stability of the AMPs with OprM, the H-bonds are analyzed using time evolution plots (Fig. 2c). The H-bonding is an important parameter in determining the interaction stabilities. The 834, 862, and 1298 show a maximum occupancy of 17, 11, and 18 H-bonds with OprM, respectively. With an average of 9 H-bonds, ~7 H-bonds remained consistent between 834 and OprM for the whole 50 ns. Similarly, with an average of 9 H-bonds, ~5 H-bonds remained consistent between 1298 and OprM for the whole 50 ns. However, with a maximum of 11 H-bonds, only ~3 H-bonds remained consistent between 862 and OprM. The results indicate that the AMPs 834, 862, and 1298 are stabilized by an average of 9, 4, and 9 H-bonds at the binding pocket of OprM.

Free Energy Landscape

The free energy landscape (FEL) plot (Fig. 3) helps us visualize the minimum energy conformational ensembles of the protein complexes aiding us in determining the conformational changes during protein-peptide interactions [29]. The Boltzmann inversion method ($F = -RT \ln P$) is used to generate the FEL plot where P signifies the probability distribution of the principal components. The FEL plots indicate that the AMPs bind with OprM along the minimum energy conformations. The FEL plot of 834 shows that the ensembles are confined to two distinct but neighboring energy basins. These two energy basins are separated by a high energy barrier of about 4.0 kcal/mol signifying stable peptide bound conformations of the OprM. As the ensembles occupy a very narrow energy basin, it is suggested that the complex readily reached stability. The FEL plot of 862 shows that the peptide navigated a vast conformational space from various energy basins. However, many of these energy minima are separated by very high energy barriers indicates that the ensemble states cannot move out from one energy basin to another easily, suggesting its conformational stability. Further, the FEL plot of 1298 shows single but elongated energy minima, suggesting its heterogeneous sub-states. With a very low energy barrier of about 1.0 kcal/mol between the ensembles, the complex is suggested to show a stable conformation within the energy basin interplaying between the sub-states.

Maximum Common Substructure

To identify the most significant protein residues that might involve in the inhibitory activity of OprM, the protein-peptide RINs of the top five docked structures are generated and analyzed. Eight common protein residues, all from chain A, are identified from the RINs. These eight common residues namely are Thr 167, Gln 174, Leu 226, Glu 277, Lys 360, Thr 364, Glu 368, and Thr 430 suggesting their importance in inhibitory activity. The residue interaction networks of the top five docked complexes are given in Fig. 4.

Further, to identify the significant inhibitory patterns from the peptides, the MCS among the top three docked complexes are analyzed. CytoMCS identified six substructures that are considered to be common among the given three RINs. The peptide residues from the substructures as identified are given in Table 2. It is observed that majorly the basic amino acids of the peptide play an important role in interacting with the commonly interacting protein residues. Further analysis suggests that the presence of basic amino acids at positions 5, 6, 9, 15, 18, and 26 to 29 of the peptides play a prominent role in inhibitory activity due to their presence in the MCS as well as their interactions with the common protein residues.

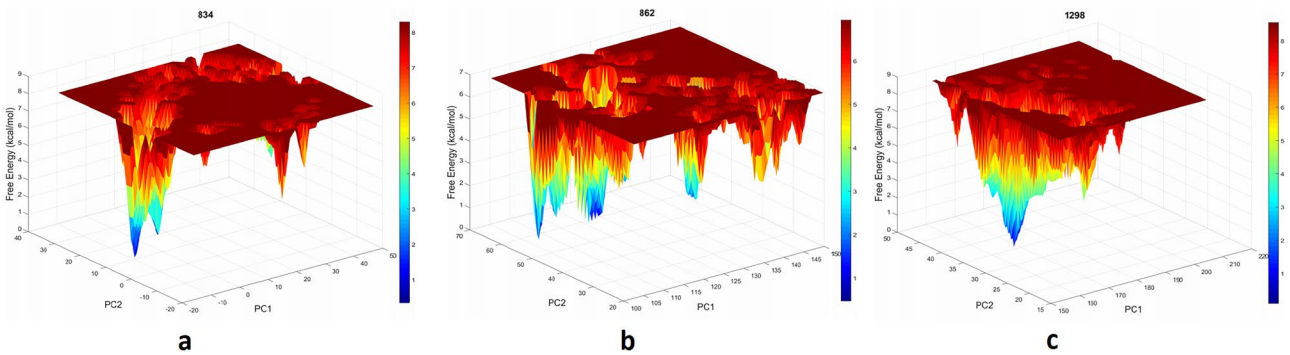

Fig. 3 FEL of OprM complexed with AMPs. **a** 834, **b** 862, and **c** 1298. The free energy is given in kcal/mol and indicated by the color code in the right panel

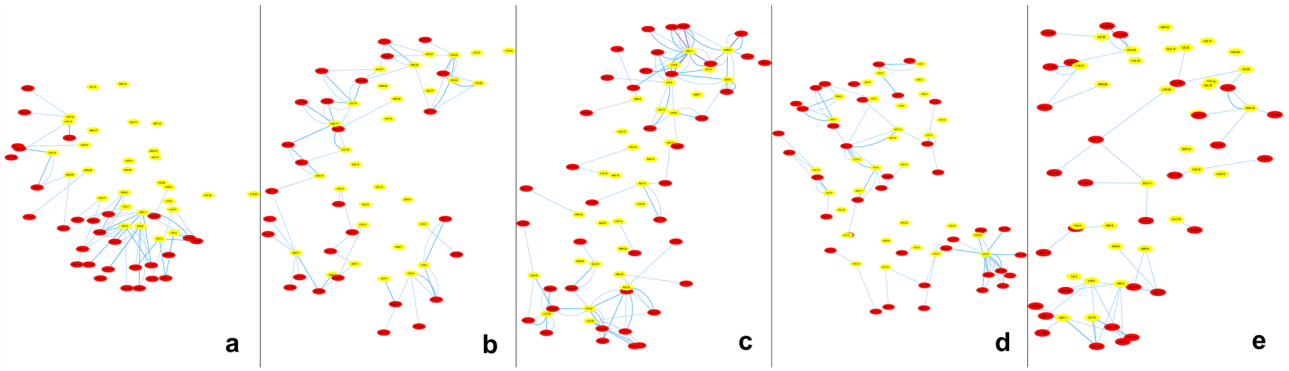

Fig. 4 The residue interaction networks of the top five docked complexes. **a** 232, **b** 834, **c** 862, **d** 1298, and **e** 1518

Table 2 The peptide residues involved in the formation maximum common substructures (MCSs)

862	834	1298
Pro 2.D	Met 1.D	Met 1.D
Ser 3.D	Ser 3.D	Lys 5.D
Gly 4.D	Lys 6.D	Lys 11.D
Lys 5.D	Lys 11.D	Met 12.D
Lys 8.D	Asn 14.D	His 15.D
Arg 9.D	Lys 18.D	Lys 18.D
His 26.D	Ala 21.D	Asn 29.D
Lys 27.D	Arg 25.D	Lys 30.D
Lys 28.D	Lys 28.D	
	Lys 29.D	

Binding Free Energy (MM-PBSA) Analysis

To investigate the molecular interaction involved in the binding and stability of AMPs to the outer membrane protein OprM, the MM-PBSA is performed to obtain a detailed analysis of the binding free energy. Results suggest that all the AMPs favorably bind to the OprM as enumerated in the supplementary file (Online Resource 1). As shown in (Fig. 5), except for LYS-360 and GLN-174, all the other common residues between the RINs especially GLU-277 and GLU-368 majorly show good binding affinity toward the peptides in the case of all three AMPs. The contribution towards negative free energy by the common residues, especially the GLN-277 and GLU-368 with an average of −261.3 kcal/mol and −292.5 kcal/mol, respectively, suggests their high significance in inhibitory activity.

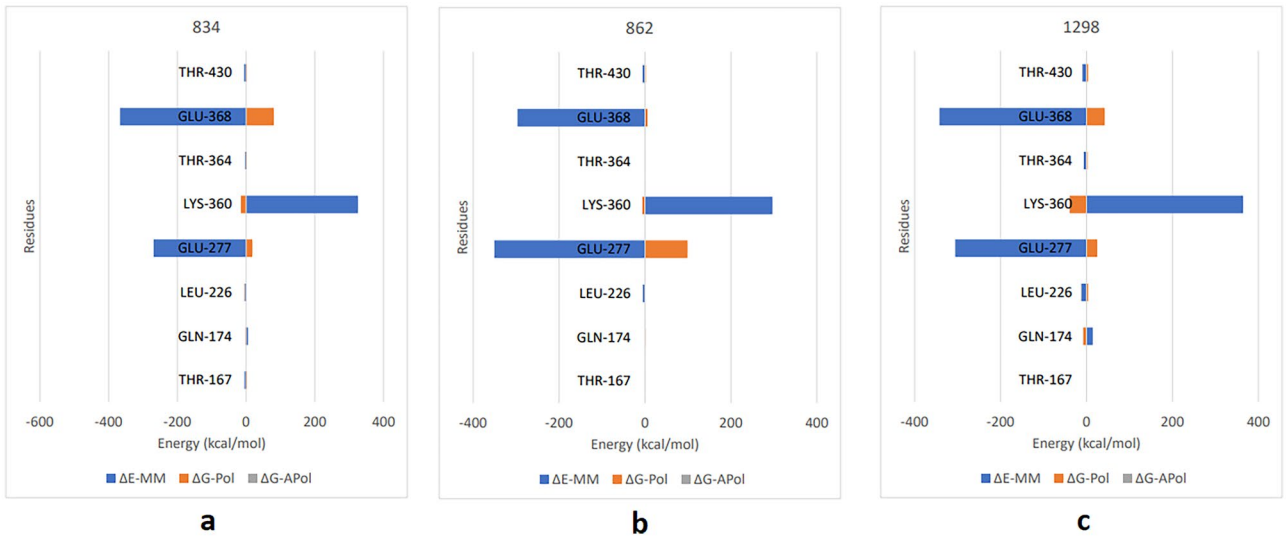

Fig. 5 The residue decomposition plot (MM-PBSA) representing the binding energy contribution of the common residues from the active site of the OprM energetically stabilizing the AMPs at the binding pocket. **a** 834, **b** 862, and **c** 1298

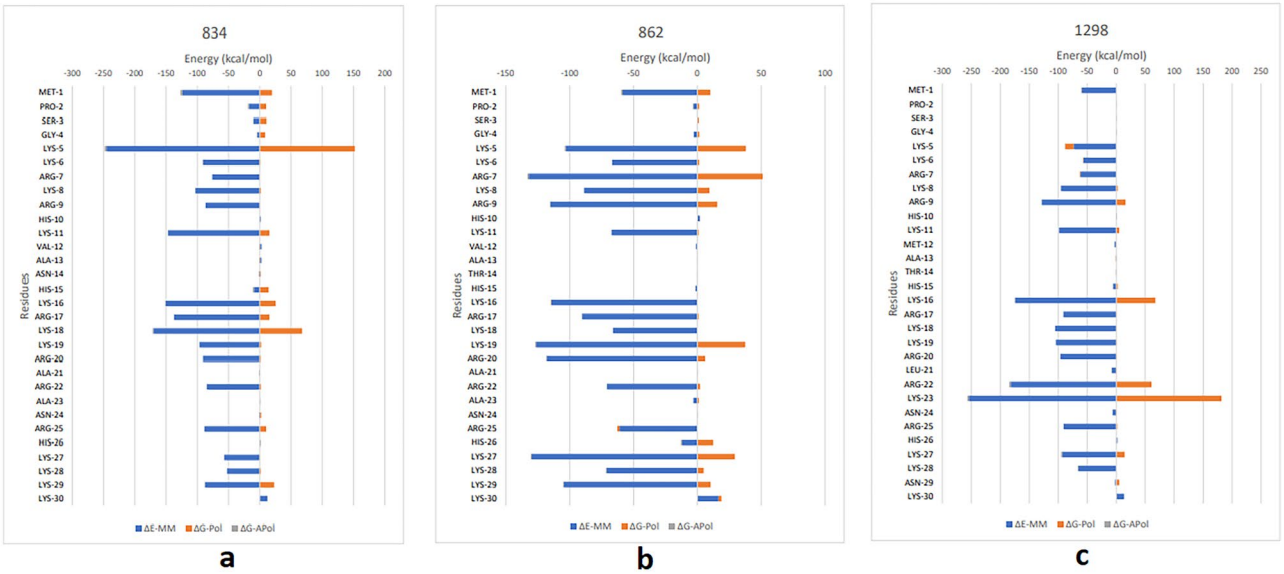

Fig. 6 The residue decomposition plot (MM-PBSA) representing the binding energy contribution of the residues from the AMPs energetically stabilizing them at the binding pocket of OprM. **a** 834, **b** 862, and **c** 1298

Further, to validate the results of the MCS that suggest the presence of basic amino acids contribute to the inhibitory activity of the peptide, the per-residue free energy contribution of the peptide is calculated using the MM-PBSA method. The per-residue free energy contribution (Fig. 6) and the MCS suggest that the basic residues of the peptide play an important role in binding to the OprM. Majorly, the basic amino acids at positions ranging from 5 to 9 and 16 to 20 contribute actively to the binding free energy with an average binding free energy of −83.8 kcal/mol and −100.4 kcal/mol, respectively.

Previous studies on the probiotics against drug-resistant bacteria suggest that the probiotics aid in mitigating drug resistance. Studies are suggesting that administration of probiotics during antibiotic treatment prevents the colonization of multidrug-resistant bacteria in the gut [30], probiotic bacteria from breastfed infant aid in inhibiting diverse multidrug-resistant bacterial strains including *Ps. aeruginosa* [31]. Supporting the effect of probiotics against pathogens, the gut microbiota imparted by the functional foods is shown to aid in the control and prevention of malaria [32]. Recent studies also suggest that designer probiotics pave a way for healthy living and efficient prevention and treatment of human diseases [33–35]. Furthering the research on the use of probiotics against drug-resistant bacteria, this study identifies the AMPs from the healthy human microbiome along with their mechanism of action against inhibiting drug resistance. While this study shows promising results regarding the composition of the AMPs that inhibit multidrug efflux pumps in *Ps. aeruginosa*, they should be further validated in an in-vitro environment to confirm their activity. These results can be used in developing a synthetic AMP against the multidrug-resistant *Ps. aeruginosa* or could be further incorporated as a part of a designer probiotic that could aid in inhibiting a broad spectrum of multidrug-resistant microbes.

Conclusion

In summary, this study explores the possibility of antimicrobial peptides from the human microbiome for their potential inhibitory effects on multidrug resistance in *Ps. aeruginosa* by inhibiting outer membrane protein OprM with is a conserved efflux pump protein in the majority of the drug resistance *Ps. aeruginosa* using computational studies. The molecular docking studies show that the majority of the AMPs from the human microbiome could efficiently bind to the drug-resistant OprM protein. Further, the RINs and the MCSs of the docked complexes are computed to identify the probable inhibitory pattern of the AMPs. To study the stability of the docked complexes and to validate the identified inhibitory patterns, the MD simulations, FELs, and per-residue free energy contributions of the OprM with AMPs are analyzed explaining the interaction stability with the vital residues in terms of H-bonding and per-residue energy estimations. Our study identifies potential AMPs against the MDR *Ps. aeruginosa* along with their mechanism of action which can be further explored as an effective inhibitor against the drug-resistant *Ps. aeruginosa*. The results conclude that the AMPs majorly consisting of basic amino acids at critical locations inhibit multidrug efflux pumps in *Ps. aeruginosa*, in turn inhibiting multidrug resistance exhibited by the bacteria.

Supplementary Information The online version contains supplementary material available at https://doi.org/10.1007/s12602-022-09910-y.

Acknowledgements The research work was carried out in the Laboratory of Chemistry, Department of Applied Sciences, Indian Institute of Information Technology Allahabad, Prayagraj, India. The Molecular Dynamic simulation results reported in this work were performed on the Central Computing Facility of IIITA, Prayagraj. V. M. is thankful to the MoE, GoI, for the fellowship to pursue a doctoral degree.

Availability of Data and Material The data generated or analyzed during this study are included in this published article and its supplementary information files.

Declarations

Conflict of Interest The authors declare no competing interests.

References

1. Sharma A, Gupta VK, Pathania R (2019) Efflux pump inhibitors for bacterial pathogens: From bench to bedside. Indian J Med Res 149:129. https://doi.org/10.4103/IJMR.IJMR_2079_17
2. Soto SM (2013) Role of efflux pumps in the antibiotic resistance of bacteria embedded in a biofilm. Virulence 4:223–229. https://doi.org/10.4161/VIRU.23724
3. Martinez JL, Fajardo A, Garmendia L et al (2009) A global view of antibiotic resistance. FEMS Microbiol Rev 33:44–65. https://doi.org/10.1111/J.1574-6976.2008.00142.X
4. Martinez JL, Sánchez MB, Martínez-Solano L et al (2009) Functional role of bacterial multidrug efflux pumps in microbial natural ecosystems. FEMS Microbiol Rev 33:430–449. https://doi.org/10.1111/J.1574-6976.2008.00157.X
5. Sberro H, Fremin BJ, Zlitni S et al (2019) Large-scale analyses of human microbiomes reveal thousands of small, novel genes. Cell 178:1245–1259.e14. https://doi.org/10.1016/J.CELL.2019.07.016
6. Bhadra P, Yan J, Li J et al (2018) AmPEP: Sequence-based prediction of antimicrobial peptides using distribution patterns of amino acid properties and random forest. Sci Rep 8:1–10. https://doi.org/10.1038/s41598-018-19752-w
7. Morrison AJ, Wenzel RP (1984) Epidemiology of infections due to *Pseudomonas aeruginosa*. Rev Infect Dis 6:S627–S642. https://doi.org/10.1093/CLINIDS/6.SUPPLEMENT_3.S627
8. Cardo D, Horan T, Andrus M et al (2004) National Nosocomial Infections Surveillance (NNIS) System Report, data summary from January 1992 through June 2004, issued October 2004. Am J Infect Control 32:470–485. https://doi.org/10.1016/J.AJIC.2004.10.001
9. Mulpuru V, Semwal R, Varadwaj PK, Mishra N (2020) HAMP: a knowledgebase of antimicrobial peptides from human microbiome. Curr Bioinforma 16:534–540. https://doi.org/10.2174/1574893615999200802041228
10. Poole K (2004) Efflux-mediated multiresistance in Gram-negative bacteria. Clin Microbiol Infect 10:12–26. https://doi.org/10.1111/J.1469-0691.2004.00763.X
11. Masuda N, Sakagawa E, Ohya S (1995) Outer membrane proteins responsible for multiple drug resistance in *Pseudomonas aeruginosa*. Antimicrob Agents Chemother 39:645–649. https://doi.org/10.1128/AAC.39.3.645
12. Tsutsumi K, Yonehara R, Ishizaka-Ikeda E et al (2019) Structures of the wild-type MexAB–OprM tripartite pump reveal its complex formation and drug efflux mechanism. Nat Commun 10:1–10. https://doi.org/10.1038/s41467-019-09463-9
13. Li XZ, Nikaido H, Poole K (1995) Role of mexA-mexB-oprM in antibiotic efflux in *Pseudomonas aeruginosa*. Antimicrob Agents Chemother 39:1948–1953. https://doi.org/10.1128/AAC.39.9.1948
14. Regberg J, Srimanee A, Langel Ü (2012) Applications of cell-penetrating peptides for tumor targeting and future cancer therapies. Pharmaceuticals 5:991–1007. https://doi.org/10.3390/PH5090991
15. Thundimadathil J (2012) Cancer treatment using peptides: current therapies and future prospects. J Amino Acids 2012:1–13. https://doi.org/10.1155/2012/967347
16. Zhang Y, Forli S, Omelchenko A, Sanner MF (2019) AutoGridFR: improvements on AutoDock affinity maps and associated software tools. J Comput Chem 40:2882–2886. https://doi.org/10.1002/JCC.26054
17. Zhang Y, Sanner MF (2019) AutoDock CrankPep: combining folding and docking to predict protein–peptide complexes. Bioinformatics 35:5121–5127. https://doi.org/10.1093/BIOINFORMATICS/BTZ459
18. Podtelezhnikov AA, Wild DL (2008) CRANKITE: A fast polypeptide backbone conformation sampler. Source Code Biol Med 3:1–7. https://doi.org/10.1186/1751-0473-3-12
19. Huang J, MacKerell AD (2013) CHARMM36 all-atom additive protein force field: Validation based on comparison to NMR data. J Comput Chem 34:2135–2145. https://doi.org/10.1002/JCC.23354
20. van der Spoel D, Lindahl E, Hess B et al (2005) GROMACS: fast, flexible, and free. J Comput Chem 26:1701–1718. https://doi.org/10.1002/JCC.20291
21. Darden T, York D, Pedersen L (1998) Particle mesh Ewald: An N·log(N) method for Ewald sums in large systems. J Chem Phys 98:10089. https://doi.org/10.1063/1.464397
22. Berendsen HJC, Postma JPM, van Gunsteren WF et al (1998) Molecular dynamics with coupling to an external bath. J Chem Phys 81:3684. https://doi.org/10.1063/1.448118
23. Maurya AK, Mulpuru V, Mishra N (2020) Discovery of novel coumarin analogs against the α-glucosidase protein target of diabetes mellitus: pharmacophore-based QSAR, Docking, and Molecular Dynamics Simulation Studies. ACS Omega 5:32234–32249. https://doi.org/10.1021/ACSOMEGA.0C03871
24. Kumari R, Kumar R, Consortium OSDD, Lynn A (2014) g_mmpbsa—a GROMACS tool for high-throughput MM-PBSA calculations. J Chem Inf Model 54:1951–1962. https://doi.org/10.1021/CI500020M
25. Cao Y, Jiang T, Girke T (2008) A maximum common substructure-based algorithm for searching and predicting drug-like compounds. Bioinformatics 24:i366–i374. https://doi.org/10.1093/BIOINFORMATICS/BTN186
26. Doncheva NT, Klein K, Domingues FS, Albrecht M (2011) Analyzing and visualizing residue networks of protein structures. Trends Biochem Sci 36:179–182. https://doi.org/10.1016/J.TIBS.2011.01.002
27. Shannon P, Markiel A, Ozier O et al (2003) Cytoscape: a software environment for integrated models of biomolecular interaction networks. Genome Res 13:2498–2504. https://doi.org/10.1101/GR.1239303
28. Larsen SJ, Baumbach J (2017) CytoMCS: a multiple maximum common subgraph detection tool for cytoscape. J Integr Bioinform 14. https://doi.org/10.1515/JIB-2017-0014
29. Boehr DD, Nussinov R, Wright PE (2009) The role of dynamic conformational ensembles in biomolecular recognition. Nat Chem Biol 5:789–796. https://doi.org/10.1038/nchembio.232
30. Wieërs G, Verbelen V, Van Den Driessche M et al (2021) Do probiotics during in-hospital antibiotic treatment prevent colonization of gut microbiota with multi-drug-resistant bacteria? A randomized placebo-controlled trial comparing saccharomyces to a mixture of lactobacillus, bifidobacterium, and saccharomyces.

Front Public Health 1039. https://doi.org/10.3389/FPUBH.2020.578089
31. Rastogi S, Mittal V, Singh A (2020) Selection of potential probiotic bacteria from exclusively breastfed infant faeces with antagonistic activity against multidrug-resistant ESKAPE pathogens. Probiotics and Antimicrobial Proteins 13:739–750. https://doi.org/10.1007/S12602-020-09724-W
32. Bamgbose T, Anvikar AR, Alberdi P et al (2021) (2021) Functional food for the stimulation of the immune system against malaria. Probiotics and Antimicrobial Proteins 13:1254–1266. https://doi.org/10.1007/S12602-021-09780-W
33. Singh B, Mal G, Marotta F (2017) Designer probiotics: paving the way to living therapeutics. Trends Biotechnol 35:679–682. https://doi.org/10.1016/J.TIBTECH.2017.04.001
34. Chua KJ, Kwok WC, Aggarwal N et al (2017) Designer probiotics for the prevention and treatment of human diseases. Curr Opin Chem Biol 40:8–16. https://doi.org/10.1016/J.CBPA.2017.04.011
35. Singh B, Mal G, Gautam SK, Mukesh M (2019) Designer probiotics: the next-gen high efficiency biotherapeutics. Advances in Animal Biotechnology 71–79. https://doi.org/10.1007/978-3-030-21309-1_7